Simulation by the Mah-3 code of the interfaces using an mixed cells and markers

N.N. Anuchina,[*] N.S. Es'kov,[*] V.A. Gordeyhuck,[*] O.M. Kozyrev,[*] V.I. Volkov[*]

[*] Russian Federal Nuclear Center – Zababakhin Institute of Technical Physics, Snezhinsk, Russia
e-mail: v.a.gordeychuk@vniitf.ru, o.m.kozyrev@vniitf.ru

The paper presents a 3D method of describing interface with unstructured mesh of markers, which is implemented in the MAH-3 code (Anuchina et al., 2004, Volkov et al., 2000).

2D and 3D test problems set-up and computed data are presented for comparison two methods: method of material mixture concentrations and markers method.

Algorithms of marker-based control the interface location in time on an Eulerian mesh and influence on calculation of convective fluids flows.

The numerical results show, that the proposed markers method allows the robust calculation of the interface location and having less error

Numerical Method

MAH-3 code is intended to calculate nonstationary 3D hydrodynamic flows of multicomponent media with strongly distorted interface.

The calculated system depending on a priori information on the problem is presented by a set of computational domains. The domain each is a topological parallelepiped. The domain boundaries may be contact or external borders of the problem. In each domain one uses a regular, arbitrary hexahedral grid of its own (Fig. 1). The radius vector $\vec{r}$ and velocity vector $\vec{u}$ are related to the cell vertices, the density ρ, the pressure p, and specific intrinsic energy e are related to the cell geometrical center. The difference method is based on splitting into Lagrangian and Eulerian stages.

In the method realized in MAX-3 the contact surfaces boundaries are described as the coordinate surfaces of the mesh in the area of numerical integration, or with the help of a triangular mesh of markers and combined cells, or by the combined cells only.

In detailed study of the contact boundary evolution the following calculation technology is used:

- At small distortions of the contact boundary it is described as a Lagrange coordinate surface of the mesh;
- At significant distortions we turn to the description of the contact boundary by means of combined cells and Lagrange triangular mesh of markers, which is not connected with the mobile Euler mesh of numerical integration area;

- In the description of turbulized flows when the contact boundaries are destroyed and there appears a zone of mixed matters, we turn to the method of concentrations.

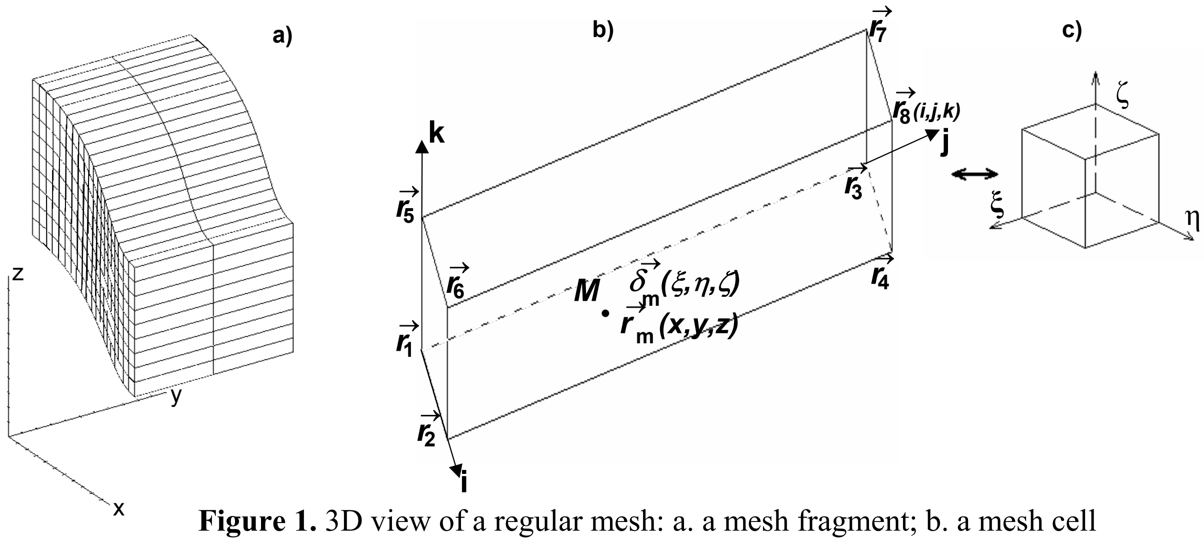

Figure 1. 3D view of a regular mesh: a. a mesh fragment; b. a mesh cell containing a marker in physical space (x,y,z); c. unit cube in a parametric space (ξ,η,ζ).

Algorithms of presentation of the surface interface as a Lagrange triangular mesh of markers

In MAX-3 method strong deformations of the matter interfaces are calculated with the help of a triangular mesh of markers. The markers show the position of the contact boundary at any moment of time. The matter interfaces may cross in an arbitrary way the Euler mesh. Here the combined cells are formed which contain several different matters. The mixture calculation is based on the conditions of hydrodynamic equilibrium of the components and continuity of the velocity vector at the contact boundary. The convective flows in the vicinity of combined cells are calculated with account for the direction of the medium flow and the composition of the matters in the cells. The matter composition in the cells is determined with the help of the markers. The calculation algorithms for strongly deformed contact boundaries with the help of a triangular mesh of markers may be divided into two groups:

- Geometrical algorithms which ensure the creation of an initial triangular mesh of markers and maintain its optimacy in the process of contact surface evolution;
- Algorithms for combined cell processing:
    - Calculation of pressure in the combined cells at the Lagrange stage,
    - Calculation of convective flows at the edges of the combined cells with account for the motion of the markers at the Euler stage.

Geometrical algorithms of the interface as a Lagrange triangular mesh of markers

Contact boundary presents a 2D surface in a 3D space. A triangular mesh is used for the description of the surface. Each nod of the mesh is a marker, and the marker motion is defined by the velocity field of the medium.

The marker is characterized by an ordinal number m, the marker cell indices (k_m, j_m, i_m), the Cartesian coordinates $\vec{r}_m(x,y,z)$ and the vector $\vec{\delta}_m(\xi,\eta,\zeta)$, where (ξ,η,ζ) are the local Lagrange coordinates of the marker with relation to the marker cell. The relation between $\vec{r}_m(x,y,z)$ and $\vec{\delta}_m(\xi,\eta,\zeta)$ is given by triangular mapping of a unity cube (fig.1.c) into 3D physical space, represented by a cell (fig.1.b) containing the considered marker:

$$\vec{r}_m(x,y,z) = (1-\xi)(1-\eta)(1-\zeta)\bullet\vec{r}_1 + \xi(1-\eta)(1-\zeta)\bullet\vec{r}_2 + (1-\xi)\eta(1-\zeta)\bullet\vec{r}_3 + \xi\eta(1-\zeta)\bullet\vec{r}_4 + (1-\xi)(1-\eta)\zeta\bullet\vec{r}_5 + \xi(1-\eta)\zeta\bullet\vec{r}_6 + (1-\xi)\eta\zeta\bullet\vec{r}_7 + \xi\eta\zeta\bullet\vec{r}_8 \Rightarrow \vec{\delta}_{\mathbf{m}}(\xi,\eta,\zeta); \quad [1]$$

$$\text{where}: \quad 0 \le \xi \le 1, \quad 0 \le \eta \le 1, \quad 0 \le \zeta \le 1$$

At the Lagrange stage the local Lagrange coordinates of the marker do not change. After the Lagrange stage the coordinates $\vec{\delta}_m(\xi,\eta,\zeta)$ are transformed into the Euler coordinates $\vec{r}_m(x,y,z)$. At the Euler stage after reconstruction of a new mesh we determine the position of the markers with relation to the cells of a new mesh, and find new local Lagrange coordinates, which in a general case do not coincide with the old ones.

The edges of the triangles define the relation between the markers at the contact surface, and this stipulates the mesh topology.

The requirements imposed on the triangular mesh of the markers are as follows:

- two neighboring markers must be located in one mesh cell or in neighboring mesh cells;
- the mesh should cover all the contact surface by nonintersecting triangles;
- the mesh should be symmetrical at a corresponding symmetry of the problem (plane, cylindrical and spherical);
- the mesh should be close to a uniform one.

Required quality of the marker mesh is supported for the account:

- addition of new markers;
- Re-mapping of the marker triangular mesh.

Creation of initial triangular mesh of markers

It is assumed that initially the contact boundary coincides with the coordinate surface of the mesh and is presented by a regular mesh composed of spatial quadrangles. When the description of the contact boundary by coordinate surface is substituted for the description by a triangular mesh of the markers the markers are placed into the nodes of a regular quadrangular mesh and geometrical centers of spatial quadrangles.

Figure 2 llustrates the principle of creation of an initial triangular mesh of the markers using the already available regular mapping of the contact boundary.

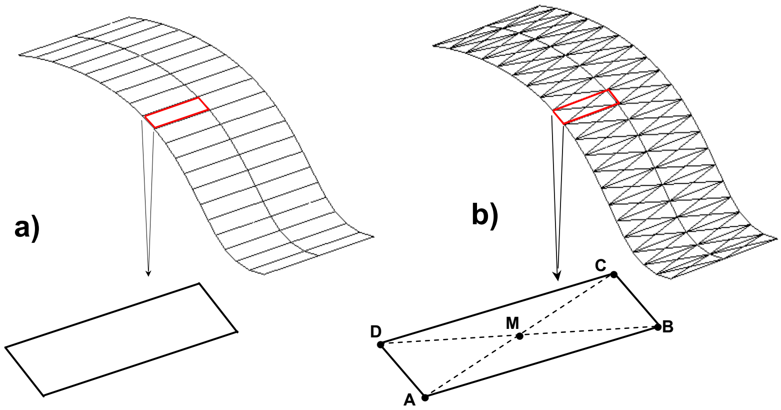

Figure 2. Mapping of an initial triangular mesh of markers at the contact boundary (and a zoomed face):
a. prior to initialization;
b. after initialization.

Addition of the marker

The mechanism of adding of a single marker is shown in fig.3. The edge AB is divided into two segments of the same length (AM, MB) and from the additional point M obtained in this way a new edge MC is plotted to the opposite vertex of the adjacent triangle. In a general case we have two such triangles: ABC и ABD.

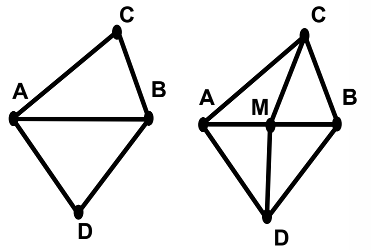

Figure 3. Addition of a new marker M.

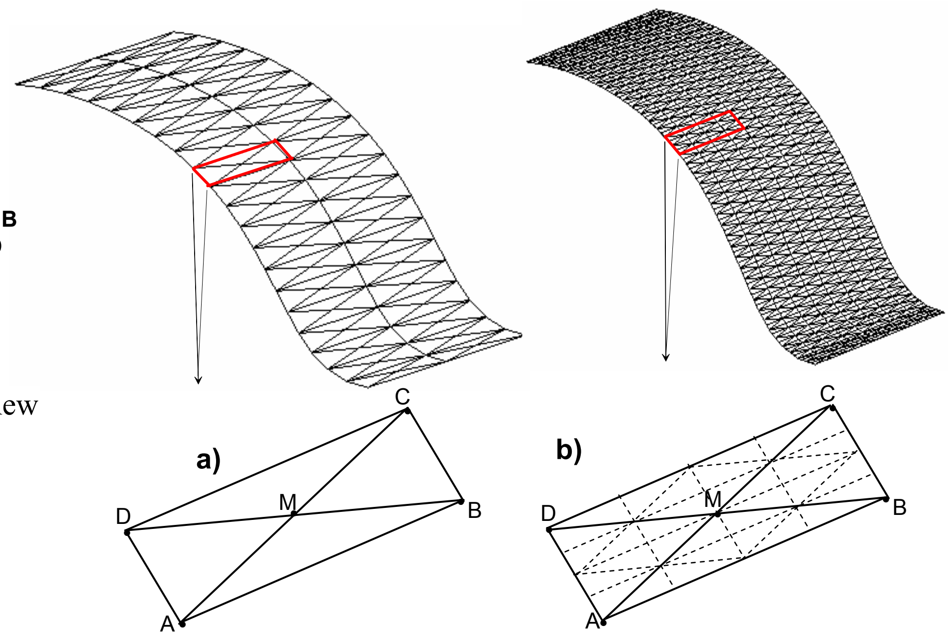

Figure 4. Example of adding new markers (and a zoomed face):
a. prior to addition; b. after addition.

Figure 4 presents an example of adding new markers on the coordinate surface. The following criterion is used when adding: distance between two points in the Lagrangian variables should be less than 0.5.

Such a simple formulation of an algorithm of the marker addition does not provide the conservation of symmetry of the numerical solution under the modeling of a corresponding symmetrical flow. So, the initial algorithm has been added by special procedures of the mesh edge sorting, and this allows one to meet the requirements on the conservation of symmetry of the numerical solution.

Figure 5 presents the projection of the contact surface onto the plane XZ with the density field and triangular mesh of markers for a plane 2D problem in which the solution does not depend on Z. The line AB separates two layers of cells over the direction Z. As the problem is two-dimensional, the position of the markers with relation to the line AB should be symmetrical. Figures 5a and 5b illustrate the calculation results obtained by an algorithm of marker addition, which conserves the symmetry of a numerical solution. Figures 5c and 5d show the results obtained by an algorithm in the initial formulation.

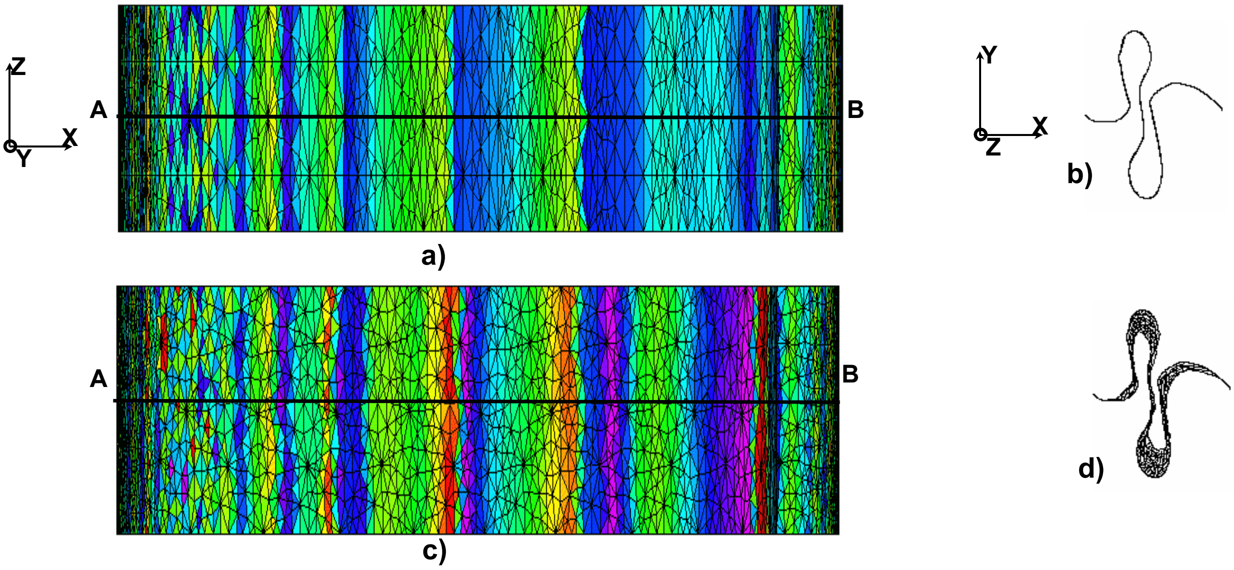

Figure 5. Conservation of symmetry in 2D calculation. 3D view mesh of markers: a., c. - Y=const; b., d. - Z=const. a), b) – the requirement of symmetry <u>is met</u>; c., d. - the requirement of symmetry <u>is not met</u>.

Re-mapping of the marker triangular mesh

In the calculation process the triangular mesh can become nonuniform. In this case the marker mesh is re-mapped. An algorithm of re-mapping is a local one and realizes the displacement of the markers in the tangent plane to the interface surface in order to equalize the distance between the neighboring markers.

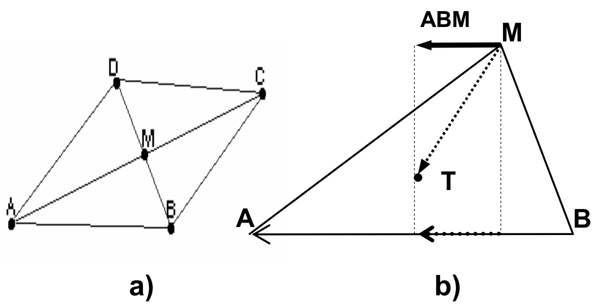

Figure 6. Remapping of M marker (for an arbitrary fragment of the triangular mesh):
a. marker and all the triangles having M as a vertex;
b. Displacement vector $d\vec{S}_{ABM}$ of M marker obtained from ABM triangle.

Fig. 6 shows as displacement vector of M marker obtained. Fig. 7 shows an interface between two substances covered by an triangular mesh of markers that is calculated without remapping (a. amount of markers is $\approx$6,500), and with remapping (b. amount of markers is $\approx$2,500).

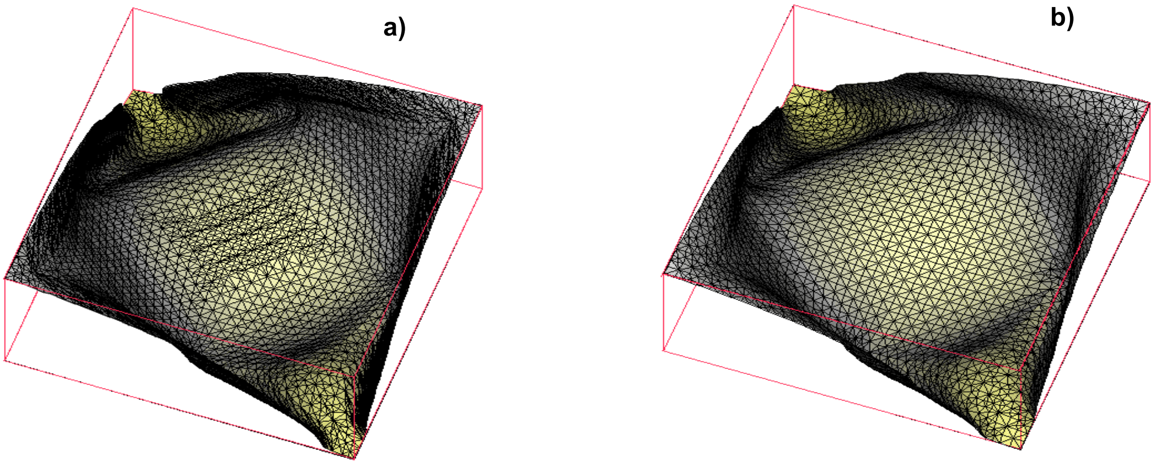

Figure 7. 3D view of unstructured triangle mesh covering the interface: a. mesh calculated without remapping; b. mesh calculated with remapping.

Processing of mixed cells

Topology of the marker triangular mesh given at the interface defines a direction of the normal. It makes the interface oriented and separates the left part of the space from the right with respect to the normal. Each interface divides the concrete matters. The direction of the normal allows to know from which side of the interface one or other matter is situated.

The matter composition of each mixed cell is defined. Each matter of the mixed cell i is characterized by the volume concentration σ_i, mass M_i, and specific intrinsic energy e_i.

Calculation of pressure in mixed cells at the Lagrangian stage

For mixed cell the total pressure and intrinsic energy of the matters of mixture are defined by a single-velocity model of a multi-component medium and the conditions of joint deformation of the components.

Let N matters be in a cell. For each matter i we know the mass M_i, the specific intrinsic energy e_i, the fraction of the volume σ_i, occupied by the matter in the cell volume V, and the equation of state of the matter $p_i = f_i(\rho_i, e_i)$ is given, where $\rho_i = M_i/(\sigma_i \cdot V)$ is the density of the matter i in the cell.

In order to calculate all the values in the mixed cell at the Lagrangian stage one should determine the pressure. In the pressure calculation we make use one of the following assumptions:

- the compression of all the mixture components should be equal;
- all the matters are of the same pressure.

In the case of the explicit difference scheme under the first assumption, and from additivity of the total intrinsic energy of the components it follows that:

$$p = \sum_i \sigma_i \cdot p_i. \qquad [2]$$

Under the second assumption the pressure p and σ_i are defined by the following system of equations:

$$\begin{aligned} & p_1 = p_2 = \ldots p_N, \\ & \sum_i \sigma_i = 1, \\ & p_i = f_i(M_i/(\sigma_i \cdot V), e_i), \end{aligned} \qquad [3]$$

which is solved by an iterative method.

If at the Lagrangian stage the implicit difference scheme is applied, the relationships above for determining pressure in the mixed cells are introduced into the iterations.

Calculation of convective flows at the faces of mixed cells with account for the marker displacement

At the next time the matter composition in the cells is determined by the analysis of the marker positions relative to a new Eulerian grid.

Each marker entering the cell of the new grid supplements its composition by the matters, which are separated by the marker surface. If all the markers come out of the cell, then, may be, only one matter will stay in the cell. This matter will be the same as in the nearest neighboring non-mixed cell, if such exists. For analysis we take only those cells, which have a common face with considered cell. If the cell does not contain markers, and the markers have not entered the cell, the matter composition is not changed.

The convective flows are calculated only between the cells having a common face. So, it is necessary to define the flows through six faces of the cell.

For each cell A we find the volume variation δV_α (Fig.8) caused by the motion of the face α resulting from the grid modification. In the case shown in Fig.8 the flow comes from the cell A into

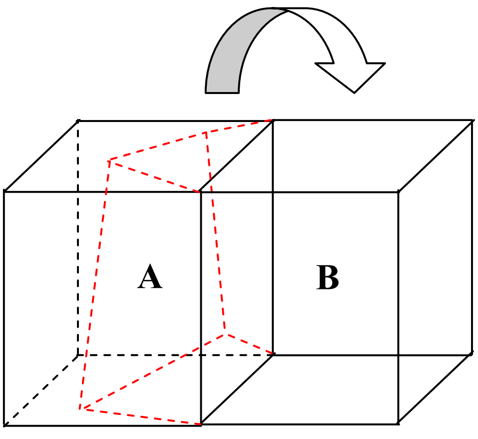

Figure 8. Calculation of flows between the cells A and B.

the cell B. In calculations it is convenient to determine only the outgoing flows for each cell.

At the beginning we define the matters participating in the fluxes and the change of their volumes. For the cells A and B both the old and new matter compositions are known. The flows from the cell A to the cell B are calculated for only those matters, which are contained in the cell A, and will be contained in the cell B.

For each matter i, flowing out from the cell A through the face α, it is necessary to determine the volume variation $\delta V_{i\alpha}$, so that $\sum_i \delta V_{i\alpha} = \delta V_\alpha$. At first for the matter i the preliminary values $\delta\tilde{V}_{i\alpha}$ are found:

$$\delta\tilde{V}_{i\alpha} = 0.5\left(\frac{\sigma_{iA}}{\sum_{i'}\sigma_{i'A}} + \frac{\sigma_{iB}}{\sum_{i'}\sigma_{i'B}}\right)\delta V_\alpha. \qquad [4]$$

Here σ_{iA} and σ_{iB} are the volume concentrations of the matter i in the cells A and B obtained at the Lagrange stage. The summation is made for all the matters flowing out from the cell A to the cell B through the face α.

After calculating the $\delta\tilde{V}_{i\alpha}$ for all the matters flowing out through all the faces of the mixed cell A, the situation is possible when the calculated volume of some matter flowing out from the mixed cell A exceeds the volume of the matter in the cell A, or is insufficient to remove any matter from the cell, although this component should not be present at the next moment of time. So, the $\delta\tilde{V}_{i\alpha}$ are corrected to obtain the final values of them. The correction is made by a redistribution of the volumes of flowing out components.

After this correction the convective flows of the mass, total energy and pulse are calculated separately for each component.

Calculation of convective flows at the faces of mixed cells by concentrations

In the description of turbulent flows, when the interfaces are destroyed and mixture of matters is formed, the method of concentrations is applied. In this case the algorithms for determination of $\delta V_{i\alpha}$ are essentially simplified and are reduced to the following.

Initially only those matters contained both in the cell A and in the cell B at the current time flow out from the cell A to the cell B. When volume of some matter calculated for all the faces exceeds its volume in the mixed cell A, then the preliminary obtained volumes of the matter are corrected at the expense of the volumes of other matters flowing out from the cell. If the latter is not a success then the rest components of the mixed cell are used.

Comparison of Marker and Concentration Methods

Problems of two types were calculated to compare two interface reconstructing algorithms, one of which is based one the concentration method and the second uses markers (i.e., an unstructured mesh of markers which move in accord with the convection flows calculated.

These included:

(1) Heterogeneous translational motion;

(2) Homogeneous translational motion.

All test problems have exact solutions.

Heterogeneous translational motion

In the calculations with the use of Eulerian methods the contact boundary (if it is not a coordinate surface) in its motion crosses the difference mesh. Here the mixed cells are formed, i.e. the cells containing several matters. The accuracy of the methods depends on the algorithms of calculation of convection flows through the mixed cell boundaries.

Interesting model problems for the comparison of different numerical methods of such type are proposed in (Rider and Kothe, 1998) for two space variables. The problems are generalized for the case of three spatial variables.

The problems have been calculated by MAX-3 code in order to compare the algorithms describing of the strong distorted interfaces: with the markers, and with the concentrations only.

Model problem for the case of two spatial variables

The motion of the points of a square $0 \le x, y \le 1$ with the velocity of $\vec{\upsilon}(u, v)$ is considered:

$$\begin{aligned} u &= -\left[\sin(\pi x)\right]^2 \sin(2\pi y)\cos(\pi t/T) \\ v &= \left[\sin(\pi y)\right]^2 \sin(2\pi x)\cos(\pi t/T) \end{aligned} \qquad [5]$$

It is seen that at the square edges $u = v = 0$, and the motion is periodic with the period T. At $t = T$ all the points return into the initial position. If at the time moment $t = 0$ we take a set of points at any curve and trace their motion then, in the process of motion, the curve is strongly deformed. Fig.9 illustrates the change of the circle shape during the motion. The greater is *T*, the stronger is the deformation. For example, at $T = 8$ during the motion the circle takes form of a spiral.

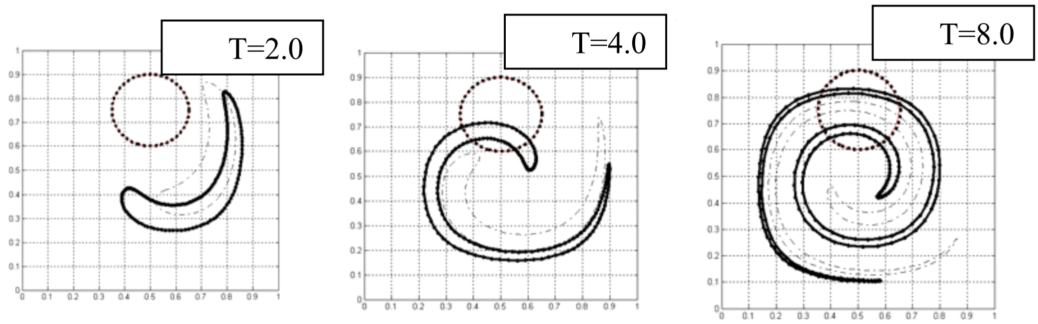

Figure 9. Change of the circle "form" for T=2, 4, 8:
- t=0, t=T; - t=0.25T, t=0.75T; - t=0.5T .

In MAH-3 simulation the formulation of the problem is as follows. Within the square $0 < x, y < 1$ with the rigid walls we consider the motion of a homogeneous incompressible liquid $(div\vec{\upsilon} = 0)$ with the above noted velocity $\vec{\upsilon}(u,v)$. The liquid parameters: $p = 0, \rho = 1$. In the liquid we separate an area where the boundary presents a circle with the radius 0.15 and the center at the point $(0.75; 0.75)$. We assume the circle to be the contact boundary between two matters.

The calculations with MAH-3 have been performed, using immobile square mesh with different number of points $(32^2, 64^2, 128^2)$, for $T = 2$ and $T = 8$ (fig.10). A peculiar feature of the problem lies in the fact that one needs to calculate only the mass flows through the boundaries of the mixed cells.

Figures 11-12 demonstrates the results obtained from the calculations by the “MM” method, which uses the marker lines for the description of the contact boundary, and the results from the method of concentrations “MC”. The mixed cells, which appear in the calculation, are shown, as well as the circle deformations obtained in the exact solution. In the “MM” calculations they coincide with the deformations of the marker lines.

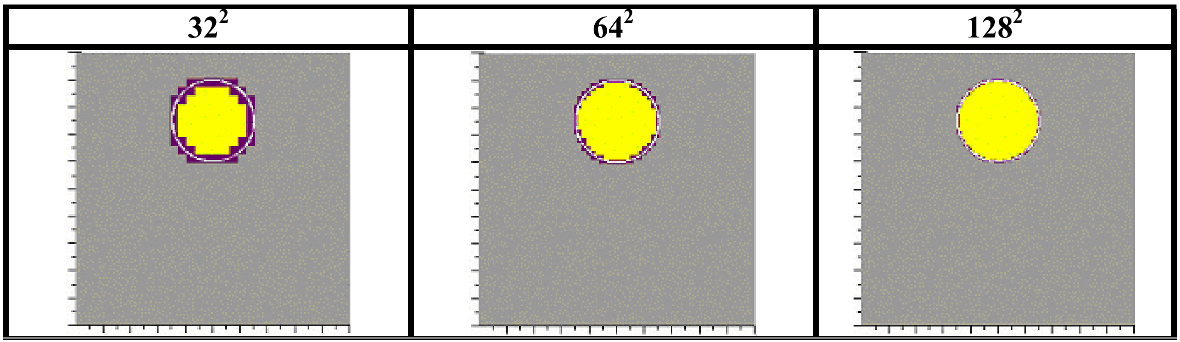

Figure 10. Initial liquid field for different number of points 32^2, 64^2, 128^2

In these calculations we tested convergence (see Tables 1, 2). At first we estimated the relative error of the volume concentration calculated for the second matter (Fig.16) with the formula $E^{L_1} = \frac{1}{V_2^{exact}} \sum_{grid, k=fix} V_{i,j,k} \left| \sigma_{2i,j,k}^{\text{computed}} - \sigma_{2i,j,k}^{\text{exact}} \right|$, where $\sigma_{2i,j,k}^{\text{exact}}$ and $\sigma_{2i,j,k}^{\text{computed}}$ are its volume fractions in the *(i, j, k)*-cell at the initial and terminal times, and $V_{i,j,k}$ is the volume of this cell. The convergence exponent α was calculated from the errors $E_1^{L_1}$ and $E_2^{L_1}$ for two different meshes spaced at steps h_1 and h_2. Since $E_1^{L_1} = \mathbb{C} h_1^{\alpha}$ and $E_2^{L_1} = \mathbb{C} h_2^{\alpha}$, where $\mathbb{C}$ is a constant, then $\alpha = \log(E_1^{L_1} / E_2^{L_1}) / \log(h_1 / h_2)$. The relative error was estimated for the calculated volume of matter 2.

$\Delta V_2 = (V_2^{\text{computed}} - V_2^{\text{exact}}) / V_2^{\text{exact}}$, where V_2^{exact} and V_2^{computed} are total initial and final volumes of matter2, respectively.

Table 1. Relative error of the matter 2 volume concentration, convergence exponent, and the relative errors in calculations for $T = 2$ with marker (MM) and concentration (MC) methods

Mesh	Error E^{L_1}		α		Error ΔV_2	
	MC	MM	MC	MM	MC	MM
32^2	0.15572	0.03339			3.532533e-004	-1.101678e-002
			0.9641	1.2247		
64^2	0.07982	0.00789			1.834880e-004	-3.460807e-003
			0.8479	1.5159		
128^2	0.04435	0.00185			9.011707e-005	-1.229808e-003

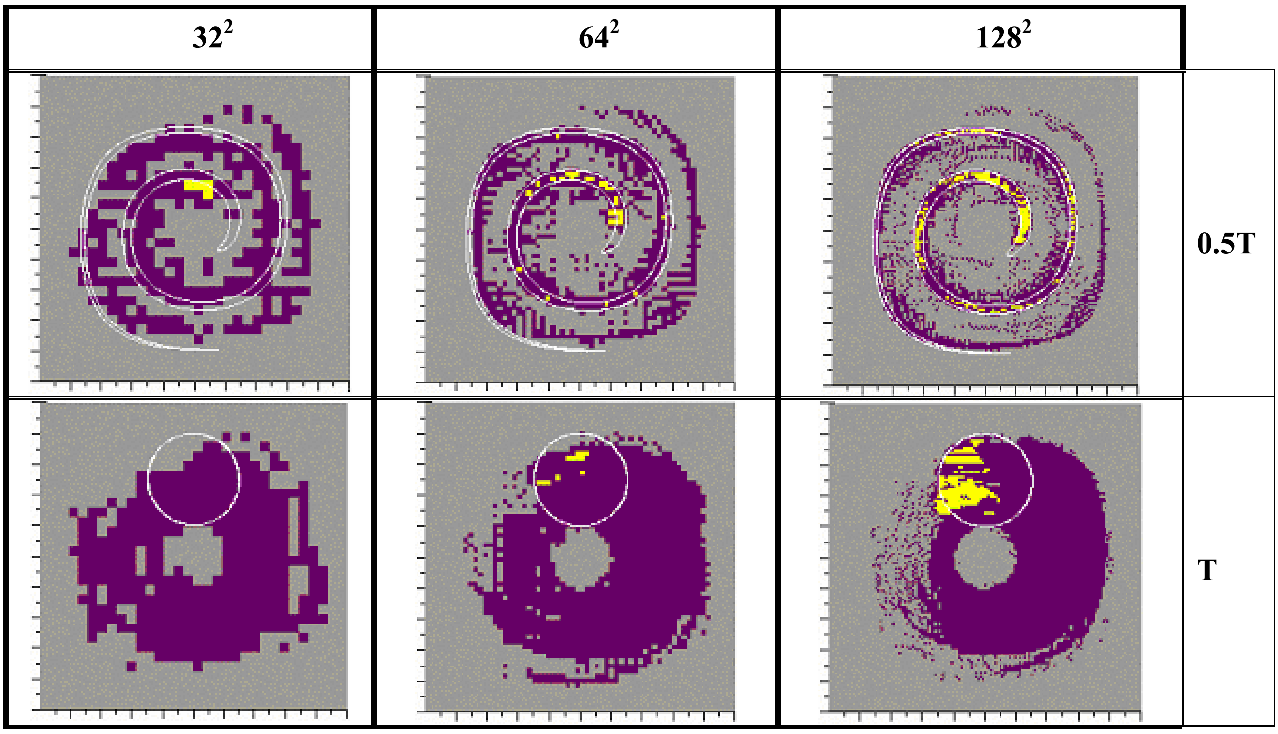

Fig.11. The results of “MC” calculation at $T = 8$ with the number of points 32^2, 64^2, 128^2 at the moments $t = 0.5\mathrm{T}$, $t = \mathrm{T}$. - matter №1; - matter №2; - mixed cells; - exact solution.

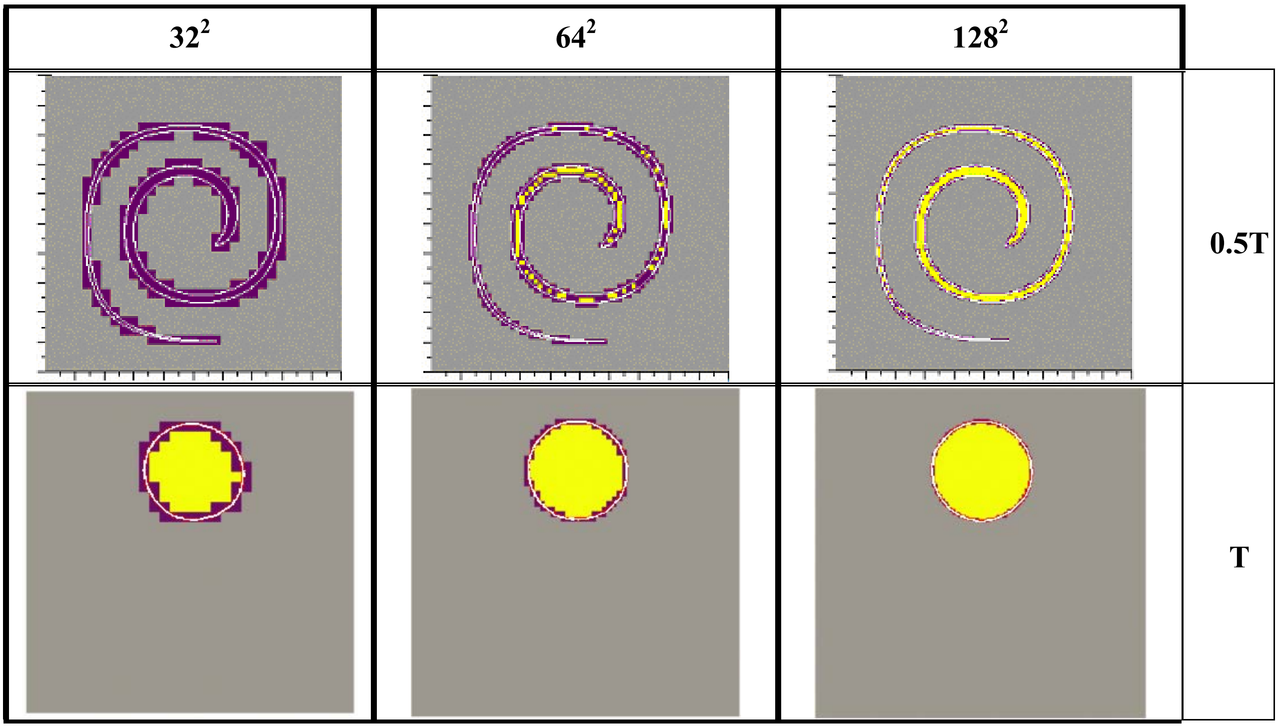

Fig.12. The results of “MM” calculation at $T = 8$ with the number of points 32^2, 64^2, 128^2 at the moments $t = 0.5\mathrm{T}$, $t = \mathrm{T}$. - matter №1; - matter №2; - mixed cells; - exact solution.

Table 2. Relative error of the matter 2 volume concentration, convergence exponent, and the relative errors in calculations for $T = 8$ with marker (MM) and concentration (MC) methods

Mesh	Error E^{L_1}		α		Error ΔV_2	
	MC	MM	MC	MM	MC	MM
32^2	1.1372	0.08308			2.561617e-003	-1.832234e-002
			0.6025	0.9577		
64^2	0.7490	0.04278			7.663488e-004	-5.355104e-003
			0.3715	0.9785		
128^2	0.57897	0.02171			4.112564e-004	-1.048725e-003

Model problem calculation for the case of three space variables

In the cube $0 \le x, y, z \le 1$ with the rigid walls there is an incompressible homogeneous liquid with the parameters $p = 0, \rho = 1$. The sphere with the radius 0.15 and the center at the point $(0.75; 0.75; 0.75)$ is assumed to be an interface separating two matters. The matter number 2 is inside the sphere, and the matter number 1 is outside the sphere.

The liquid moves with the velocity $\vec{\upsilon}(u, v, w)$:

$$u = \left[\sin(\pi x)\right]^2 \sin(2\pi y)\cos(\pi t/T)$$
$$v = \left[\sin(\pi y)\right]^2 \sin(2\pi x)\cos(\pi t/T) \qquad [6]$$
$$w = -2\left[\sin(\pi z)\right]^2 \sin(2\pi x)\sin(2\pi y)\cos(\pi t/T), \text{ i.e. } div\vec{\upsilon} = 0.$$

In the comparative calculations performing by MAH-3 code with $T = 2$ and $T = 8$ an immovable Eulerian grid in which the number of cells equal to 32^3 was used.

Figures 13-15 show the initial distribution of the sphere matter and calculated results.

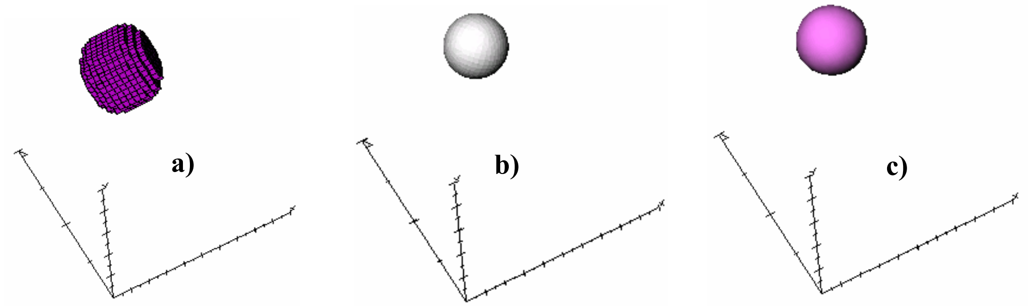

Figure 13. Initial sphere matter distribution: a) mixed cells; b) marker surface; c) isosurface with the volume concentration of the second matter $\sigma = 0.23$

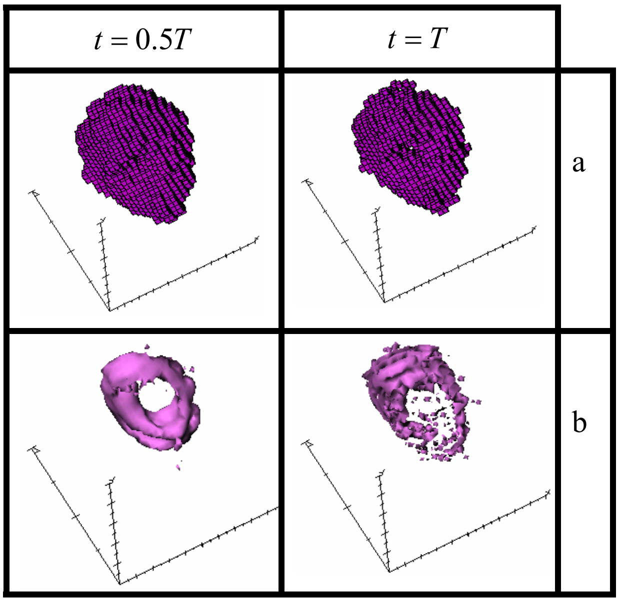

Fig.14. The results of "MC" calculation at $T = 8$: a - mixed cells; b – surfaces where the volume concentration of the second matter is $\sigma = 0.23$

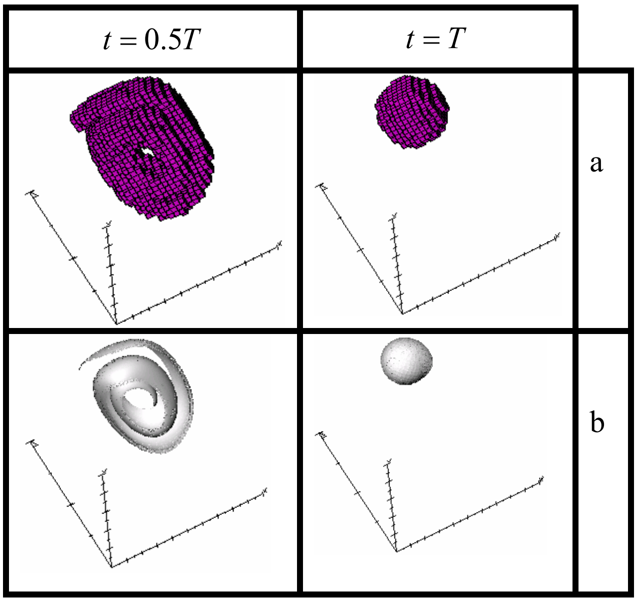

Fig.15. The results of "MM" calculation at $T = 8$: a - mixed cells; b - marker surface.

The comparative calculations show that the calculation diffusion with describing the interface by the marker surfaces is essentially smaller. In the method of concentrations a rather difficult problem is to reconstruct the interface position by the concentration field. In the considered calculations the problem is simplified by the fact that the exact solutions are known. A series of tests in the processing of 3D calculations ("MC") at $T = 2$ gives a rather good agreement with the exact solution, if we assume as a contact boundary an iso-surface with the volume concentration of the second matter $\sigma = 0.23$. For $T = 8$, where the deformations are stronger, the same processing gives much worse results.

In these calculations we also estimated the relative error in the calculated volume concentration of matter in the sphere $E^{L_1} = \frac{1}{V_2^{exact}} \sum_{grid} V_{i,j,k} \left| \sigma_{2i,j,k}^{\text{computed}} - \sigma_{2i,j,k}^{\text{exact}} \right|$ and the relative error in the calculated volume of the sphere $\Delta V_2 = (V_2^{\text{computed}} - V_2^{\text{exact}}) / V_2^{\text{exact}}$ (see Table 3).

Table 3. Погрешности при расчете сферического жидкостного тела, помещенного в обращаемое по времени течение с периодом T на момент времени $t = T$ для расчетов по методу концентраций (MC) и методу маркеров (MM)

Problem		Errors E^{L_1}	Errors ΔV_2
$T = 2$	MC	0.37922237	+8.629715e-004
	MM	0.12949270	-2.562035e-002
$T = 8$	MC	1.40545132	+6.825963e-003
	MM	0.26338374	-8.044026e-002

However, it should be noted that there are the problems where the method of concentrations gives acceptable results. For the problems with strong deformations of the contact boundaries it is best to use a set of different algorithms of description. As noted above, such a possibility is realized in MAX-3 complex. For example, in studying the instability development at the matter interface the following technology is used: the contact boundary is described by a coordinate surface at small deformations, at strong deformations – by the marker surface, and at boundary destruction and matter mixing – only by the concentrations.

Homogeneous translational motion

Model problem for the case of two spatial variables

The square $0 < x < 400$, $0 < y < 400$ contains two matters of the same pressures $p_1 = p_2 = 0$, but different densities $\rho_1 = 1, \rho_2 = 10$.

The initial geometry of the second matter - is a square 40x40 with the beginning in a point (80, 80).

We considered the matter motion with a constant velocity:

For the first calculation, $\vec{u}_0 = (1,0)$ - the motion along the (mesh) line up to the moment t = 200;

For the second calculation, $\vec{u}_0 = (0.7071, 0.7071)$ - the motion along the main diagonal up to the moment t ≈ 212.132.

At some of the square edges the matter inflow with the velocity $\vec{u}_0$ was given, and he matter outflow was given through other edges of the square.

The calculation was performed in immobile cubic Eulerian mesh with the cells size $h_x = h_y = 5$. The interface was described by the marker surface.

EOS: P = 0; time step ≈ 0.1, i.e., $|\vec{u}| \bullet \tau / h \approx 0.02$, where $\vec{u}$ = velocity, τ = time step, h = cell length.

Two calculations were done in the same setup but with another geometry of the second material defined as a circle of radius R=25 centered at $(100,100)$.

In these calculations we estimated the relative errors in the calculated volume concentration of the second material: $E^{L_1} = \frac{1}{V_2^{exact}} \sum_{grid,k=fix} V_{i,j,k} \left| \sigma_{2i,j,k}^{\text{computed}} - \sigma_{2i,j,k}^{\text{exact}} \right|$, where $\sigma_{2i,j,k}^{\text{exact}}$ and $\sigma_{2i,j,k}^{\text{computed}}$ are volume fractions of material 2 in the *(i, j, k)*-th cell at initial and final times, $V_{i,j,k}$ is the volume of this cell, and the relative error in the calculated volume of material 2 $\Delta V_2 = (V_2^{\text{computed}} - V_2^{\text{exact}}) / V_2^{\text{exact}}$, where V_2^{exact} and V_2^{computed} are the total initial and final volumes of material 2, respectively.

Results obtained with concentrations (MC) and markers (MM) are compared in Table 4 and Fig.16, where:

A) – the motion of the square along mesh lines;

B) – the motion of the circle along mesh lines;

C) – the motion of the square at an angle to mesh lines;

D) – the motion of the circle at an angle to mesh lines.

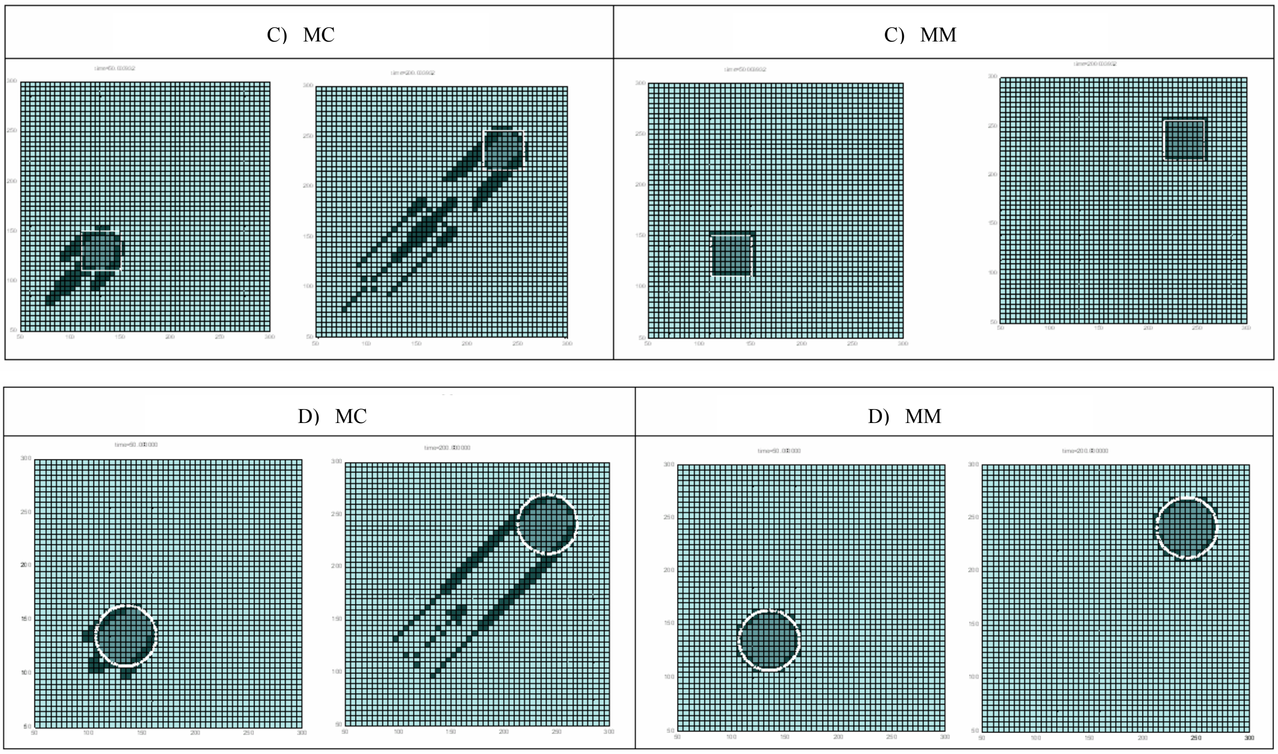

Figure 16. Homogeneous translational motion in 2D case. Matters field, mixed cells (black) and markers (white) at t = 50 and at the termination time.

Table 4. Errors E^{L_1} and ΔV_2 at the final moment

Problem		Errors E^{L_1}	Errors ΔV_2
A)	MC	0.04845338	0
	MM	1.2500e-008	0
B)	MC	0.09840140	-3.700217e-006
	MM	0.03411712	-1.705050e-006
C)	MC	0.32989223	0
	MM	0.01542336	-0.00468230341
D)	MC	0.13162436	0
	MM	0.03880181	-0.02768624309

Model problem calculation for the case of three space variables

The cube $0 < x, y, z < 2$ contains two matters of the same pressures $p_1 = p_2 = 0$, $p_1 = p_2 = 0$, but different densities - $\rho_1 = 1, \rho_2 = 10$. The initial geometry of the second matter presents a sphere of the radius of 0.15 and the center in the point $(0.25, 0.25, 0.25)$. We considered the matter motion with a constant velocity:

For the first calculation, $\vec{u}_0 = (1,0,0)$ - motion along mesh lines till t=1;

For the second calculation, $\vec{u}_0 = (0.5775, 0.5775, 0.5775)$ - motion at an angle to mesh lines (along the main diagnal) till t=2.5.

At some of the cube edges the matter inflow with the velocity $\vec{u}_0$ was given, and the matter outflow was given through other edges of the cube.

Calculations were done with a fixed cubic mesh $64 \times 64 \times 64$. The interface was described by a marker surface.

Two 3D calculations were done in the same setup but with the following modifications: integration region $350 < x, y, z < 350$; material 2 was shaped as a cube $40 \le x, y, z \le 40$; the first calculation was run to t=200 and the second one to t=300.

Calculations were done with a fixed cubic mesh $70 \times 70 \times 70$. The interface was described by a marker surface.

Figure 17 shows results for the motion along the main diagonal.

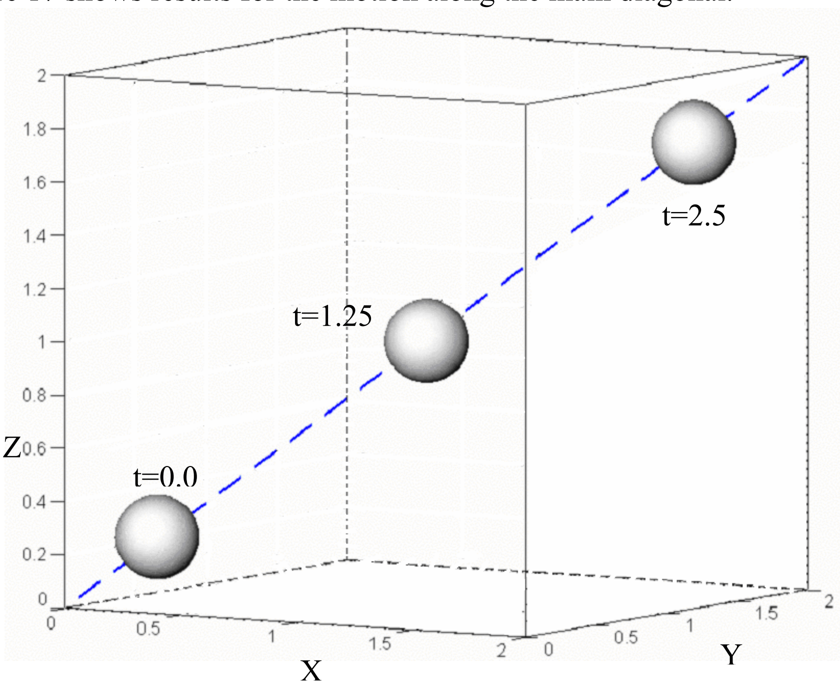

Fig.17. Position of the interface (presented by a marker mesh) at different times for the motion along the main diagonal (the initial geometry of the second matter presents a sphere).

In these calculations we estimated the relative errors in the calculated volume concentration of the second material: $E^{L_1} = \frac{1}{V_2^{exact}} \sum_{grid} V_{i,j,k} \left| \sigma_{2i,j,k}^{\text{computed}} - \sigma_{2i,j,k}^{\text{exact}} \right|$, where $\sigma_{2i,j,k}^{\text{exact}}$ and $\sigma_{2i,j,k}^{\text{computed}}$ are volume fractions of material 2 in the *(i, j, k)*-th cell at initial and final times, $V_{i,j,k}$ is the volume of this cell, and the relative error in the calculated volume of material 2 $\Delta V_2 = (V_2^{\text{computed}} - V_2^{\text{exact}}) / V_2^{\text{exact}}$, where V_2^{exact} and V_2^{computed} the total initial and final volumes of material 2, respectively.

Table 5 contains results obtained with concentration (MC) and markers (MM):

A) – the motion of the cube along mesh lines;

B) – the motion of the sphere along mesh lines;

C) – the motion of the cube at an angle to mesh lines;

D) – the motion of the sphere at an angle to mesh lines.

Table 5. Errors E^{L_1} and ΔV_2 at the final moment

Problem		Errors E^{L_1}	Errors ΔV_2
A)	MC	0.04587	0
	MM	1.7278e-005	0
B)	MC	0.15116	0
	MM	0.12405	0
C)	MC	0.65902	0
	MM	0.04358	-0.01365
D)	MC	0.90081	0
	MM	0.11380	-0.026589

Conclusion

Our calculations show that despite some shortcomings (longer (1-20%) computation time) the method of markers offers some advantages.

The method of markers reconstructs interfaces very accurately.

It tracks volumes more accurately and improves the convergence exponent approximately by a factor of 1.5.

References

Anuchina N.N., Volkov V.J., Gordeychuk V.A., Es'kov N.S., Ilytina O.S., Kozurev O.M. Numerical simulation of Rayleigh-Taylor and Richtmyer-Meshkov instability using MAX-3 code. *Journal of Computational and Applied Mathematics*, vol. 168 (2004), pp. 11-20.

Volkov V.I., Gordeychuk V.A., Es'kov N.S., Kozyrev O.M. Numerical simulation by the MAH-3 code of the interfaces using an unstructured mesh of markers. *Laser and Particle Beams*,18 (2000), pp.197

W.J. Rider, D.B. Kothe, Reconstructing volume tracking, *J. Comput. Phys*. 141 (1998) 112-152.